Problem Chosen	2022 ShuWei Cup Summary Sheet	Team Control Number
D		2022110713591

Triple La Nina Event Loss Assessment and coping strategies

Summary

In the Equatorial Middle East Pacific, La Niña are associated with lower water temperatures and stronger trade winds. So the La Niña is actually a product of the interaction of the tropical ocean and the atmosphere. In the equatorial middle-east Pacific, the atmosphere and the ocean are coupled by the exchange of heat, water vapor and momentum at the interface, and the movement of the ocean surface is mainly controlled by the surface wind. The formation of tropical latitudinal circulation (Walker) . When la Nina event occurs, the equatorial trade winds will strengthen further, the cold water upwelling in the Peruvian coastal waters will continue to strengthen, and the tropical zonal circulation will strengthen significantly. When an El Niño event occurs, the equatorial trade winds weaken and the deep convective zone over Asia and Indonesia moves eastward, forming the opposite Walker circulation. This paper is based on this research.

For question one, in order to predict the probability of future triple La Niña events, the statistical analysis of precipitation and temperature changes in the major countries and regions of the triple La Niña events was carried out, a multi-step LSTM time series prediction model is established, the influence of sudden flow is considered, the structure of neural network is further designed and improved, and the structure of LSTM network considering many external factors is constructed. We first process the abnormal data, then use Haar wavelet transform to predict the time series mutation, and combined with multi-layer LSTM model to predict. Finally, we introduce an adaptive Particle swarm optimization (PSO-RRB- algorithm to reduce the dependence of hidden layer neurons on the firing time series and the training set, so as to speed up the convergence of the model training process and improve the prediction efficiency as much as possible, predicting a triple la Nina event in the future.

For question two, we collected precipitation, annual change of sea level, total reservoir capacity, permanent population, GDP and economic loss data of an area, and quantified the above-mentioned main influencing factors based on the data processing techniques of multiple interpolation, based on factor analysis method, the loss assessment model of high temperature and drought disaster in triple la Nina event was established. Finally, by solving the model, the regional comprehensive score from 2010 to 2022 is obtained. To verify the robustness of the model, we performed a sensitivity analysis

For question three, we select Precipitation, Change in sea level over year, Drain pipe length, Total reservoir capacity, Permanent population and GDP as the evaluation factors of flood disaster loss assessment model caused by SANLA Niña event, in this paper, the correlation analysis of these evaluation factors, and finally the use of gray prediction algorithm for flood disaster losses to predict the final results

For question four, this article reports on The causes of La Nina and La Nina triggers regional or global climate anomalies.

Keywords: Multi-layer LSTM model, Factor Analysis, Correlation Analysis, grey correlation

Contents

1 Introduction

1.1 Problem Background

The latest data from the World Meteorological Organization show that the already prolonged La Nina event is likely to continue through the end of the year or beyond, which would be the first "triple" La Nina event in the 21st century -- three consecutive La Nina winters in the Northern Hemisphere. A La Nina event is a continuation of unusually cold sea surface temperatures in the eastern and central equatorial Pacific Ocean.

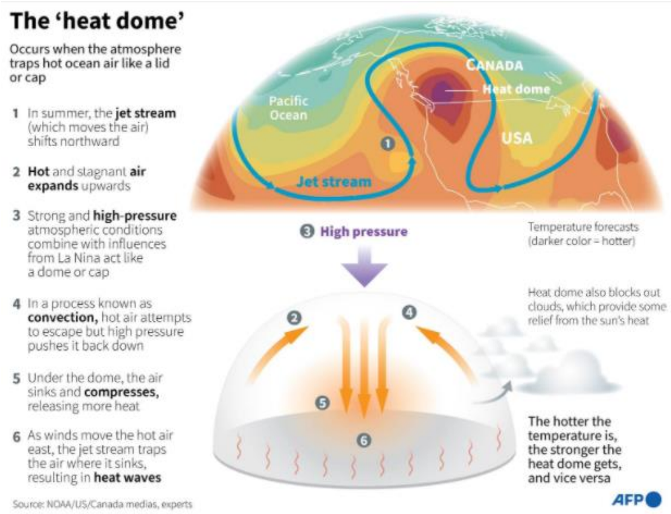

Figure.1: Global Climate

La Nina is associated with cooler water temperatures and stronger trade winds in the equatorial Middle Eastern Pacific. So La Nina is actually the product of a combination of the tropical ocean and atmosphere. In the equatorial Middle East Pacific, the atmosphere and ocean are coupled together through the exchange of heat, water vapor and momentum at the interface, and the movement of the ocean surface is mainly controlled by the surface wind. The equatorial winds from the northern and southern hemispheres blow the warm surface water westward, which not only increases the depth of the 20℃ isotherm of the subsurface water of the western Pacific Ocean, but also provides energy for the convection and rise of the air over Asia and Indonesia. The upper air flow returns to the eastern Pacific, and appears to sink, forming the tropical latitude circle (Walker) circulation. When La Nina events occur, the equatorial trade winds will be further strengthened, the cold water upwelling of the ocean off the coast of Peru will be continuously strengthened, and the tropical latitudinal circulation will be significantly strengthened. When an El Nino event occurs, the equatorial trade winds weaken and the deep convection zone over Asia and Indonesia moves eastward, forming the opposite Walker circulation. This paper is based on this research.

1.2 Clarification and Restatement

Given the background information and constraints identified in the problem statement we need to address the following questions:

- Problem 1: Conduct statistical analysis of the major countries and regions involved in the global Triple La Niña event, and predict the possibility of the Triple La Niña events in the future.

- Problem 2: Taking a country as an example, evaluate and analyze the various types of disaster losses caused by heat and drought under the Triple La Niña event, and provide targeted coping strategies.
- Problem 3: Taking a country as an example，evaluate and analyze various disaster losses caused by floods under the action of the Triple La Niña event, and provide targeted coping strategies.
- Problem 4: Please write a report of no more than 2,000 words for the relevant management in response to the Triple La Niña Event.

1.3 Problem analysis

1.3.1 Analysis of question one

Firstly, in order to predict the probability of future triple La Niña events, the statistical analysis of precipitation and temperature changes in the major countries and regions of the triple La Niña events was carried out, a multi-step LSTM time series prediction model is established, the influence of sudden flow is considered, the structure of neural network is further designed and improved, and the structure of LSTM network considering many external factors is constructed. We first process the abnormal data, then use Haar wavelet transform to predict the time series mutation, and combined with multi-layer LSTM model to predict. Finally, we introduce an adaptive Particle swarm optimization (PSO-RRB- algorithm to reduce the dependence of hidden layer neurons on the firing time series and the training set, so as to speed up the convergence of the model training process and improve the prediction efficiency as much as possible, predicting a triple la Nina event in the future.

1.3.2 Analysis of question two

Firstly, we collected precipitation, annual change of sea level, total reservoir capacity, permanent population, GDP and economic loss data of an area, and quantified the above-mentioned main influencing factors based on the data processing techniques of multiple interpolation, based on factor analysis method, the loss assessment model of high temperature and drought disaster in triple la Nina event was established. Finally, by solving the model, the regional comprehensive score from 2010 to 2022 is obtained. To verify the robustness of the model, we performed a sensitivity analysis.

1.3.3 Analysis of question three

Firstly, we select Precipitation, Change in sea level over year, Drain pipe length, Total reservoir capacity, Permanent population and GDP as the evaluation factors of flood disaster loss assessment model caused by SANLA Niña event, in this paper, the correlation analysis of these evaluation factors, and finally the use of gray prediction algorithm for flood disaster losses to predict the final results.

1.3.4 Analysis of question four

Firstly, this article reports on The causes of La Nina and La Nina triggers regional or global climate anomalies.

1.4 Our Work

The full flow chart is as follows：

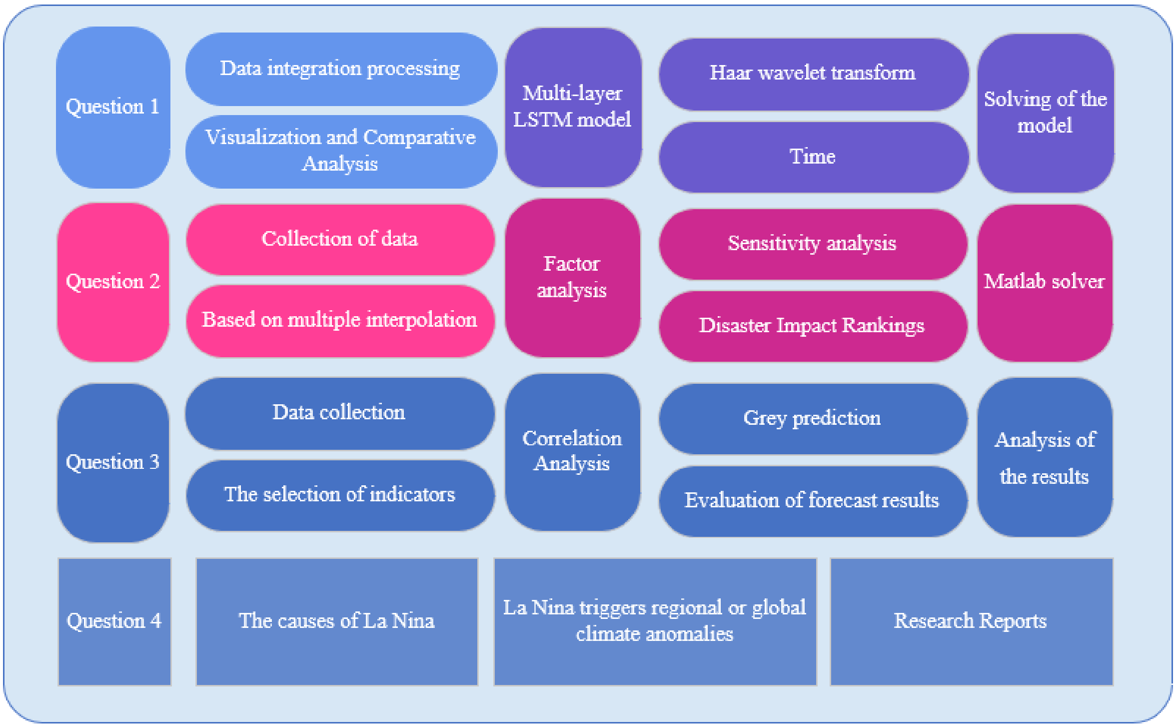

Figure.1: Work

Note: The full text flowchart is an explanation of the work in the full text

2 Model assumptions

In order to simplify the model, we make some general assumptions.

- We assume that these data are sufficient to assess La Nina events and complete model training.
- We assume that these data provide a more realistic and effective way to assess the impact of La Nina events.

3 Notations

Symbol	Description
X1	Precipitation /mm
X2	Change in sea level over year /mm
X3	Drain pipe length /km
X4	Total reservoir capacity / 10,000 cubic meters
X5	Permanent population / 10,000
X6	GDP / 100 million yuan

* See the text for other symbols

4 Model

4.1 Task 1: Multi-level LSTM time series prediction model based on Multi-Step

4.1.1 Collection of Data

We used quarterly data from the Oceanic Index Niño (ONI) of the ENSO cycles of 1950–2020, provided by the National Oceanic and Atmospheric Administration (NOAA). ENSO cycles in the tropical Pacifc Ocean are detected by diferent methods, including satellite remote sensing, sea level analysis, and by anchored, foating, and disposable buoys (Climate Prediction Center, 2012). ONI is NOAA's main indicator for monitoring LN and EN. It tracks mean sea surface temperatures (SSTs) quarterly in the eastern-central tropical Pacifc, called as Niño index 3.4 (5° N and 5° S in latitude and 170 to 120° W in longitude), as proposed by Trenberth (1997) (Fig. 1). The ENSO is characterized based on the date which the events were mature/seasoned. The SST, in 125 m deep, carries relevant information and provides a source for predicting the extent of the ENSO in advance (Pinault, 2016). Niño 3.4 region is important to delimit the study area since it is accepted that ENSO exhib its a diferent behavior when observed in the central and/or eastern Pacifc regions (Kao and Yu, 2009) The data visualization is shown below

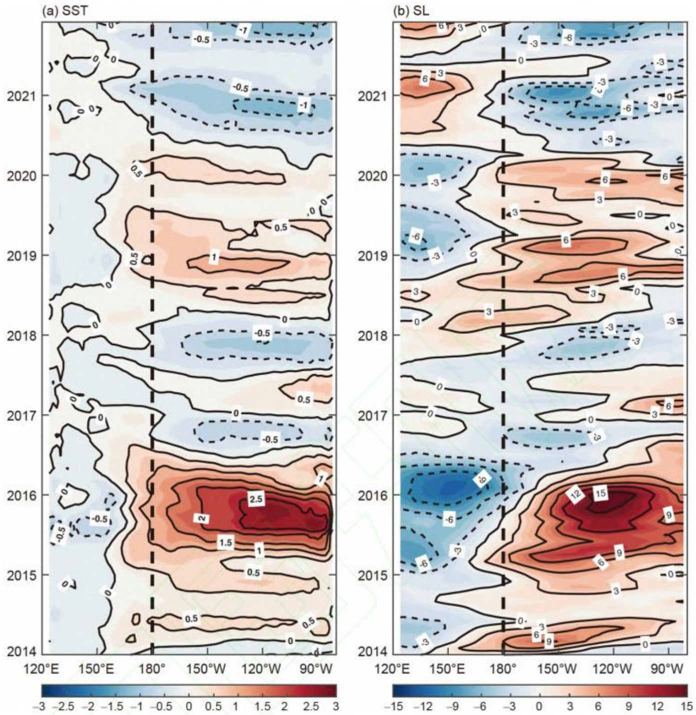

Figure.2 Data visualization

The above results show that from August 2020 to now, SST in the equatorial Middle East Pacific has been in a low state. Especially in autumn and winter 2020, autumn and winter 2021 and autumn and winter this year, SST near these three time points is significantly lower, that is, there are three process "lows", which span three winters. Hence the name "triple" La Nina event.

4.1.2 Spatial distribution of temperature and precipitation trends

Spatial variability of annual mean temperature in the middle and lower reaches of the Yangtze River.

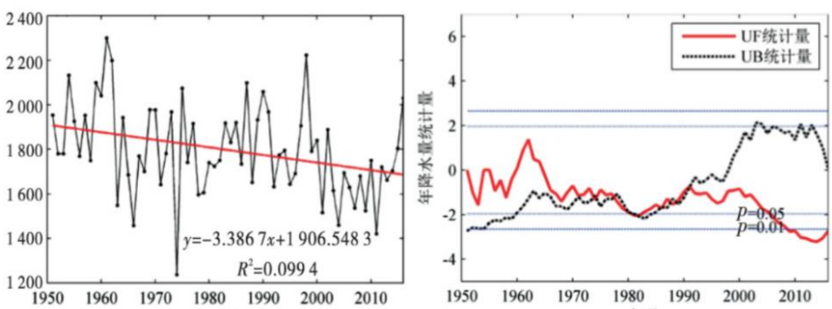

Figure.3: (a) Linear regression of annual precipitation and (b) MK test

As can be seen from the figure above, the growth trend gradually strengthened from south to north, especially in northern Hubei, northwestern Anhui and northern Jiangsu Province. The temperature change in some areas is not synchronized with the whole region, and the southwest of Hunan Province even shows a decreasing trend. Overall, the temperature increase in the south of the Yangtze River is less than that in the north of the Yangtze River, and that in the west of the region is less than that in the east. The spatial distribution of precipitation decreases gradually from northwest to southeast, and the average annual decrease of rainfall in the northwest of the middle and lower reaches of the Yangtze River is more than 10mm, especially in Hubei Province (FIG. 3b). The precipitation in the southern part of Hunan and the southern part of Jiangxi showed an upward trend, while the precipitation in the eastern coastal areas also decreased but not significantly. In conclusion, under the background that the middle and lower reaches of the Yangtze River tend to be warm and dry as a whole, the northwest and the north of the Yangtze River have the most significant trend, while the southwest is dry but the temperature rise is not obvious.

Regional temperature and precipitation visualization is shown in the figure below:

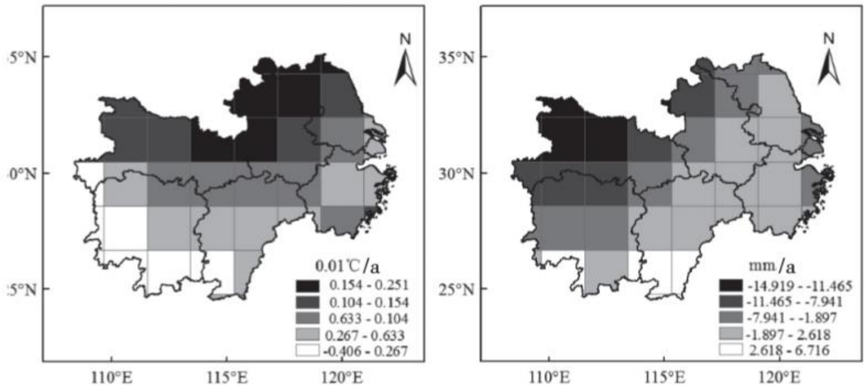

Figure.4: Regional temperature and precipitation visualization

4.1.3 The establishment of multi-layer LSTM time series prediction model based on Multi-Step

We select the short-term information that can be deeply learned in time series, construct a deep neural network that conforms to its change pattern, and further determine it as Long and Short term memory neural network (LSTM), mainly based on its advantages as follows

(1) With self-learning function. It is expected that the future deep neural network LSTM can make use of computer technology for long-term sequence prediction and time prediction, with high self-adaptation ability, and can continuously predict the traffic trend by deep learning.

(2) It has the ability to find the optimal solution at high speed. Long term prediction often requires a lot of computation. By constructing the feedback multi-layer LSTM network model, the high-speed computing ability of the computer can be brought into play and the optimization solution can be found quickly.

So we establish based on Multi - Step of multilayer LSTM deep learning time series model, first of all to adjust unit of time, due to forecast for a long time, we chose the recursive type strategy, at the same time, analysis the influence of other factors, this period of time as the network input factors, coupled with the improved particle swarm algorithm to speed up the model calculation.

4.1.4 LSTM network structure

LSTM is an improved network formed by adding long and short-term memory units to the hidden layer of recurrent neural network, including forgetting gate, input gate and output gate, to control the use of historical information. Its network structure is shown in the figure below:

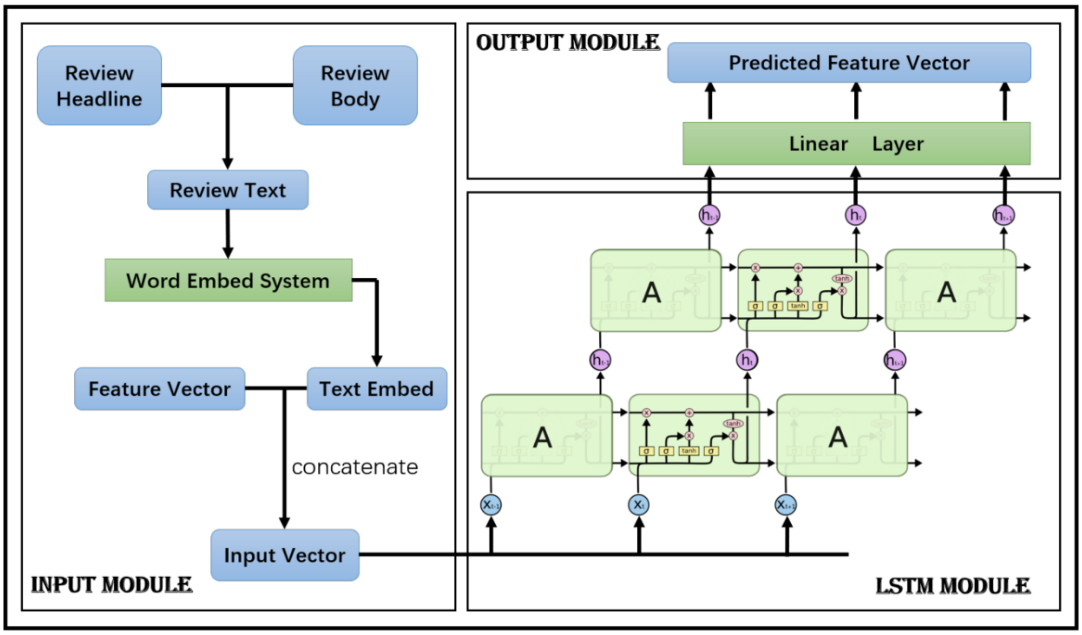

Figure.5: Improved LSTM network structure

In the figure above, is the long-term state input, is the short-term state input, and is the output of the forgetting gate, transmitting part of the time series discarded or deleted at the last moment . After entering the short-term state, four input gate structures were set up respectively, where, and are mutation prediction; Is ordinary sequence prediction, and the corresponding excitation function is tanh.

After entering the long-term state, deep neural network prediction is carried out. When the error tolerance is met, the next step is to replace the short-term sequence and output the prediction information. Meanwhile, the short-term state information at the last moment is combined with the long-term state information through the forgetting gate to form the current long-term state information of LSTM. When the error tolerance is not satisfied, the feedback signal is transmitted to both ends respectively, and the error function is transmitted in the training stage, and then the LSTM network is predicted again.

Considering the prominent influence of the external environment on basic education, we set up multiple activation functions to predict the mutation amount when constructing the LSTM network input gate, so that the final model is more suitable for the complex actual situation.

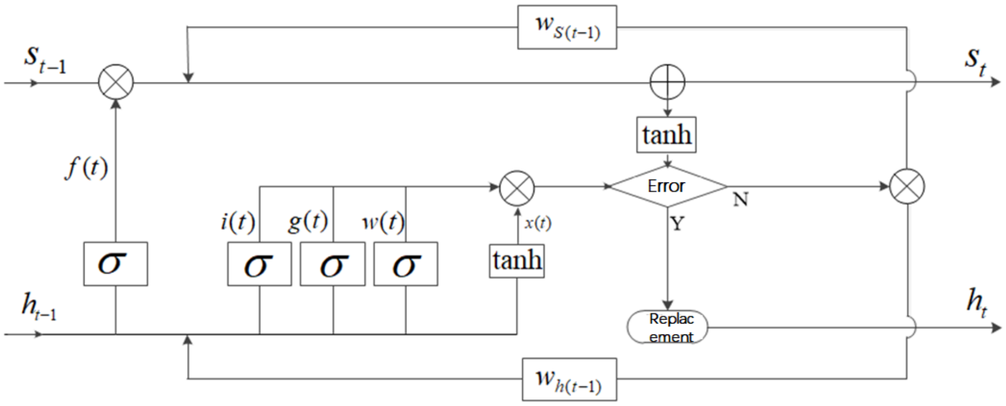

Figure.6: Flow chart of LSTM algorithm

Assuming that the hidden layer weight coefficient and bias term of the input gate are respectively the hidden layer weight coefficient and bias term of the output layer, then the forward algorithm process used by LSTM for prediction is

(1) Calculation formula of forgetting door

$$f(t) = \sigma(U_f h_{t-1} + b_f) \tag{1}$$

(2) Input gate calculation formula

$$i(t) = \sigma(U_i h_{t-1} + b_i) \tag{2}$$

$$g(t) = \sigma(U_g h_{t-1} + b_g) \tag{3}$$

$$w(t) = \sigma(U_w h_{t-1} + b_w) \tag{4}$$

$$x(t) = \tanh(U_x h_{t-1} + b_x) \tag{5}$$

$$x(t) = \tanh(U_x h_{t-1} + b_x) \tag{6}$$

(3) Output gate calculation formula

$$h_t = \tanh(s_{t-1}) + i(t) + g(t) + w(t) + x(t) \tag{7}$$

Where, the input Sigmoid function and the output tanh function are obtained by taking derivatives respectively.

$$\begin{cases} \sigma(z) = y = \dfrac{1}{1+e^{-z}}; \sigma'(z) = y(1-y) \\ \tanh(z) = y = \dfrac{e^z - e^{-z}}{e^z + e^{-z}}; \tanh'(z) = 1 - y^2 \end{cases} \tag{8}$$

Finally, after a complete LSTM calculation, the output value is the predicted value of the target.

4.1.5 Results of the model

The prediction results of the model are as follows:

Table 1: Prediction results

year	Precipitation/mm	Annual average winter precipitation /mm	Temperature / ℃	Average winter temperature over the years /℃
1964	2.5	5.8	-8.1	-8.1
1970	10.8	5.8	-10.8	-8.1
1973	4.8	5.8	-9.1	-8.1

1975	10. 4	5. 8	−8. 8	−8. 1
1984	6. 2	5. 8	−10. 1	−8. 1
1988	11. 9	5. 8	−8. 3	−8. 1
1995	2. 3	5. 8	−9. 5	−8. 1
1998	0. 1	5. 8	−6. 2	−8. 1
1999	3	5. 8	−9. 3	−8. 1
2000	3. 6	5. 8	−6. 1	−8. 1
2007	9. 9	5. 8	−9. 9	-8.1
2010	6. 6	5. 8	−8. 7	−8. 1
2011	1.8	5.8	-9.2	-8.1
2017	4.3	5.8	-8	-8.1

The visualization of prediction results is shown in the figure below

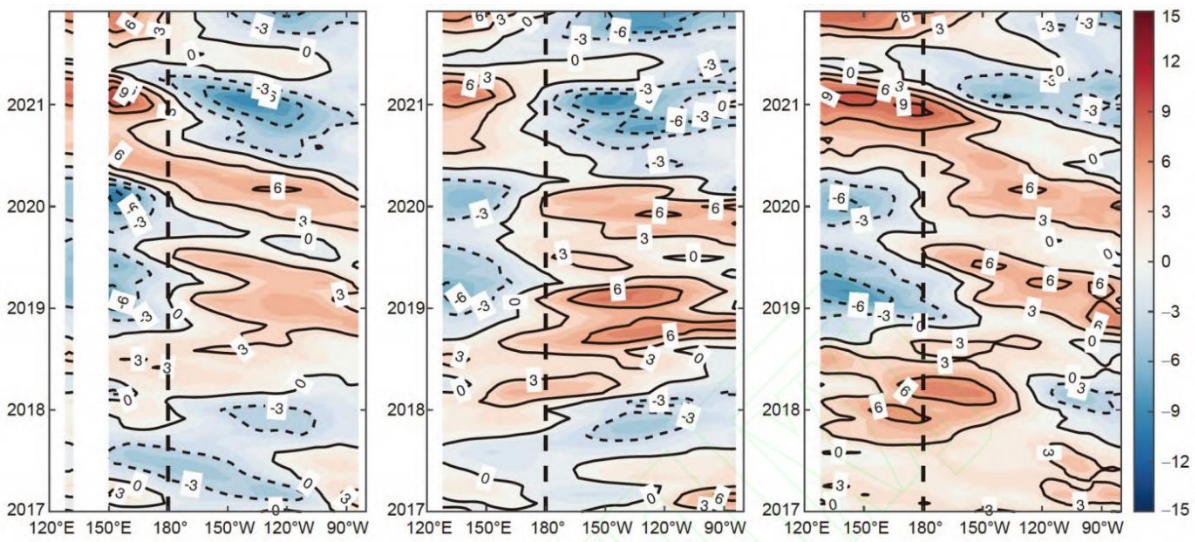

Figure.7: Visualization of prediction Results

4.2 Task 2: Damage assessment model of high temperature and drought disasters based on factor analysis

4.2.1 Description of data

The data used in this study include direct economic loss data, socio-economic data, meteorological station data and model data of drought in North China from 1984 to 2014. The data of direct economic losses from drought from 1984 to 2014 were derived from China Meteorological Disaster Yearbook. Social and economic data are based on the data of 1984-2014 for the whole country and provinces (cities and regions), including CPI, rural per capita disposable income and rural population of provinces (cities and regions). The meteorological observation data are the monthly precipitation data of 91 meteorological stations in North China from 1984 to 2014. The data are provided by the National Meteorological Information Center and data quality control is carried out. The data are interpolated and superimposed by the climatic field and the anomaly field respectively, and the generated resolution is 0. 5° x 0. 5° gridded data. See figure for distribution of weather stations in North China

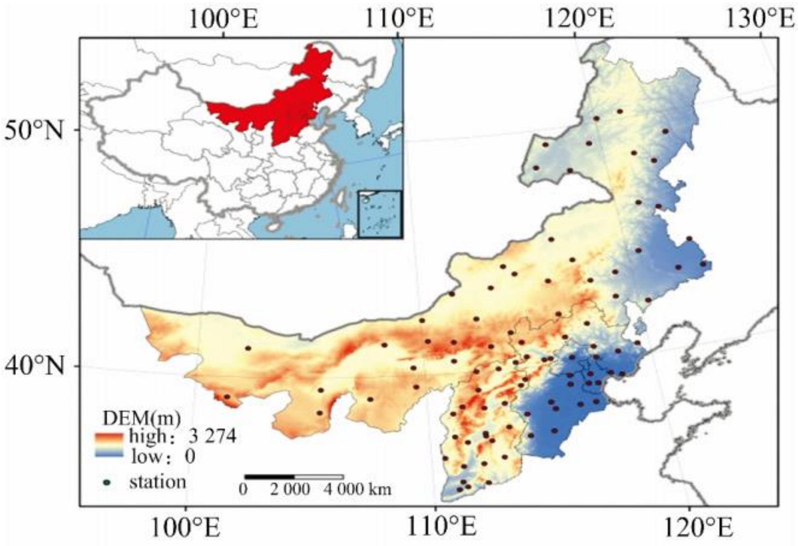

Figure.8: Distribution of meteorological stations in North China

The variation trend of precipitation is shown in the figure below:

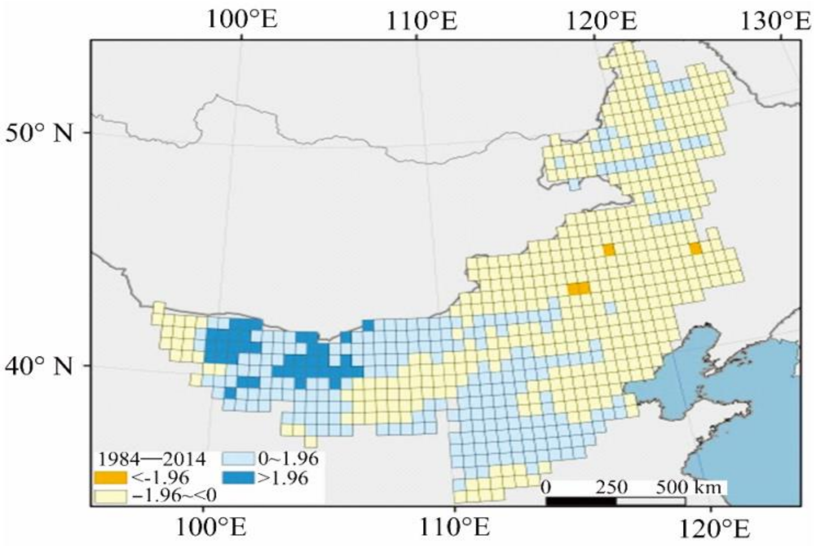

Figure.9: Variation trend of precipitation

4.2.2 Damage assessment model of high temperature and drought disasters based on factor analysis

1. Method analysis and model construction

Factor analysis is a multivariate statistical analysis method with the core idea of data transformation and dimensionality reduction. Complex variables are first combined into several main factors, and then comprehensively interpreted or evaluated. The starting point of factor analysis is the correlation matrix of the original variables. Factor analysis can be conducted by transforming various disaster losses caused by high temperature and drought of triple La Nina events into several factors, and selecting major factors according to certain criteria to eliminate the correlation between variables for evaluation and analysis.

Firstly, six relevant indicators are selected to calculate the correlation coefficient matrix among them. After removing some indicators with low correlation, precipitation x1, annual change of sea level x2, total reservoir capacity x3, permanent population x4, GDPx5 and economic loss x6 are selected as six factor indicators. Using factor analysis, each variable can be represented by k (k>p) factor lines, and the mathematical model is established as follows:

$$\begin{cases} x_1 = \alpha_{11} f_1 + \alpha_{12} f_2 + \alpha_{13} f_3 + \ldots \alpha_{1k} f_k + \theta_1 \\ x_2 = \alpha_{21} f_1 + \alpha_{22} f_2 + \alpha_{23} f_3 + \ldots \alpha_{2k} f_k + \theta_2 \\ x_p = \alpha_{p1} f_1 + \alpha_{p2} f_2 + \alpha_{p3} f_3 + \ldots \alpha_{pk} f_k + \theta_p \end{cases} \tag{9}$$

where f denotes the common factor and x is the original variable after normalization; α is the factor loading matrix. And αij(i=1,2,3... .k,j=1,2,3... .p); α_{ij} is the covariance of f_i with x_i.

2. Solving of the model

(1) Calculate the correlation coefficient matrix

The quantitative analysis model of precipitation based on factor analysis is established by using SPSS software, and solved by using SPSS. At the same time, the specific quantitative analysis of triple La Nina events is carried out. Finally, replace the data of six indicators, and use SPSS software to calculate the correlation coefficient between indicators. The calculation results are shown in the following table.

Table 2: Indicator correlation coefficient matrix

	X1	X2	X3	X4	X5	X6
X1	1	0.164	0.049	-0.007	0.257	0.164
X2	0.164	1	0.029	-0.041	0.502	0.049
X3	0.049	0.029	1	-0.945	0.080	-0.007
X4	-0.007	-0.041	-0.945	1	-0.097	0.257
X5	0.257	0.502	0.080	-0.097	1	0.073
X6	0.073	0.331	-0.006	0.007	0.230	1

The table shows that most of the correlation coefficients between the six indicators are larger than 0.5, such as precipitation and the indicators of the correlation coefficient is larger, only a few indicators of the correlation coefficient between the low impact of the model.

(2) KM0 test and Bartlett's spherical test

The KMO test statistic is used to compare the correlation coefficients and bias correlation coefficients between the variables with the following statistic.

$$KMO = \frac{\sum\sum_{i \neq j} r_{ij}^2}{\sum\sum_{i \neq j} r_{ij}^2 + \sum\sum_{i \neq j} p_{ij}^2} \tag{10}$$

where r_{ij} is the correlation coefficient between variables x_i and x_j, and p_{ij} is the partial correlation coefficient between variables xi and xj. The statistic takes values in the range of [0,1]. the closer the KMO is to 1, the stronger the correlation of the variables and the more suitable for factor analysis.

The Bartlett's spherical test statistic was obtained from the correlation coefficient matrix of the original variables, which approximately obeyed the chi-square distribution. If the chi-square value is significant and P is less than 0.05, the original hypothesis is rejected, indicating that there is correlation between the variables, i.e., the original variables are suitable for factor analysis. Conversely, if it is approximately 0.05, it means that factor analysis is not suitable.

Table 3: KM0 test and Bartlett's spherical test

KMO sampling suitability quantity		0.597
Bartlett's sphericity test	Approximate cardinality	3088.785
	Degree of freedom	36
	Significance	0.000

From the table, it can be seen that the KMO takes a value of 0.597, which indicates that the correlation between the variables is strong and can be subjected to factor analysis. The Bartlett's spherical test in order to see whether the data come from a total that obeys a multivariate normal distribution, the significant value in the table is 0.00, which indicates that the data come from a normally distributed total and is suitable for further analysis.

（3）Selection of principal components

Only the first 4 eigenvalues are greater than 1 in the column of "initial eigenvalues", so we only extract the first 4 principal components; the variance of the first 3 columns of "extracted sum of squares loaded" accounts for 79.586% of the variance of all the principal components, thus it can be seen that The first 4 principal components are sufficient to replace the original variables and can cover almost all the information of the original variables.

$$\begin{cases} w_1 = 0.24587 \\ w_2 = 0.22361 \\ w_3 = 0.19437 \\ w_4 = 0.13201 \end{cases} \tag{11}$$

Table 4: Total variance explained

Ingredients	Initial Eigenvalue			Extraction of the sum of squares of loads			Sum of squared rotating loads
	Total	Percentage of variance	Cumulative %	Total	Percentage of variance	Cumulative %	Total
1	2.213	24.587	24.587	2.213	24.587	24.587	2.187
2	2.013	22.361	46.948	2.013	22.361	46.948	1.951
3	1.749	19.437	66.385	1.749	19.437	66.385	1.753
4	1.188	13.201	79.587	1.188	13.201	79.587	1.271
5	0.723	8.034	87.621	/	/	/	/
6	0.005	0.056	100.000	/	/	/	/

Extraction method for principal component analysis

The gravel map is obtained as shown in the following figure：

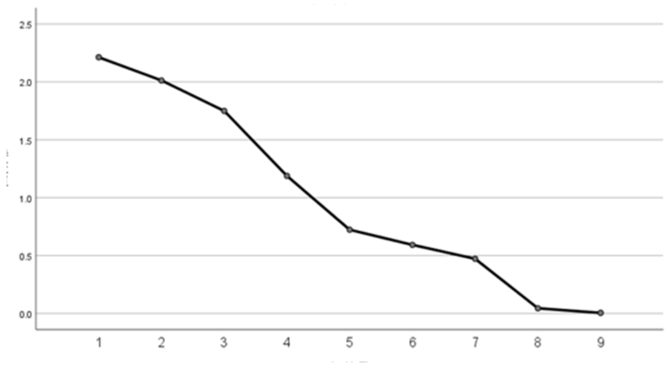

Figure.10 Gravel map

（4）Calculation of common factor equation and composite factor score formula

This leads to the equation for the four common factors.

Using the composite factor score formula.

$$F = w_1F_1 + w_2F_2 + w_3F_3 + w_4F_4 \tag{12}$$

（5）Results of the model

Table 5: Top 20 years of precipitation

Ranking	1	2	3	4	5
Year	1981	2001	1963	1987	2007
Ranking	6	7	8	9	10
Year	2005	2008	2011	1982	2006
Ranking	11	12	13	14	15
Year	2019	2015	1988	2003	2012
Ranking	16	17	18	19	20
Year	2016	1984	1985	1985	2014

4.3 Task 3: Based on spearman-grey forecasting model for flood disaster loss assessment

4.3.1 Spearman correlation coefficient method

Spilman rank correlation is a way to study the correlation between two variables based on rank data. It is calculated from the difference between pairs of pairs of pairs of pairs of ranks, and Spilman's rank correlation is not as strict about the data conditions as the product-difference correlation coefficient, as long as the observations of the two variables are paired rating data, or are transformed from the observations of continuous variables, regardless of the overall distribution of the two variables, the size of the sample size, can Be studied using Spilman's rank correlation.

Spilman's correlation coefficient can be derived from the following equation:

$$\rho = \frac{\sum_{i=1}^{n}(x_i - \bar{x})(y_i - \bar{y})}{\sqrt{\sum_{i=1}^{n}(x_i - \bar{x})^2 \sum_{i=1}^{n}(y_i - \bar{y})^2}} \tag{13}$$

Where n is the sample size, P is the correlation coefficient, and X and y are the corresponding elements in the two variables.

The correlation coefficients between rainfall, sea level change, drainage pipes, total reservoir capacity, resident population, GDP and triple La Niña events are calculated as follows:

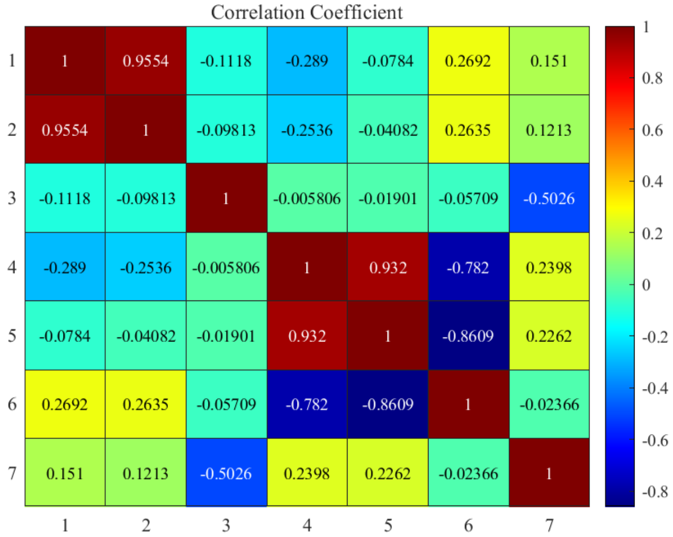

Figure.11 Correlation coefficient matrix thermodynamic diagram

4.4 The disaster loss model based on grey prediction

Through the analysis of the results, it is found that the predicted data error is large. In this paper, the grey prediction model is used to optimize the classification statistical model.

4.4.1 The establishment of disaster loss model based on GM (1,1) algorithm

Gray Forecast Model is a kind of forecasting method that establishes mathematical Model and makes Forecast through a little and incomplete information. The structure variable prediction system is a typical grey system, which has the good characteristic of using“Few data” to seek the law of reality and overcomes the defect of insufficient data, so we can use the grey GM -LRB-1,1) model.

The sequence of parameters is as follows:

$$X^{(0)} = \left\{\left(x^{(0)}(1), x^{(0)}(2), x^{(0)}(3), \dots, x^{(0)}(48)\right)\right\} x^{(0)}(i) \geq 0, (i = 1, 2, 3, \dots, 48) \tag{14}$$

To make an accumulative generating sequence:

$$X^{(1)} = \left\{\left(x^{(1)}(1), x^{(1)}(2), x^{(1)}(3), \dots, x^{(1)}(48)\right)\right\} \tag{15}$$

Among them:

$$X^{(1)}(i) = \sum_{k=1}^{i} X^{(0)}(k) \tag{16}$$

Using the differential equation to establish the GM (1,1) albino form:

$$\frac{dX^{(1)}}{dt}+aX^{(1)}=u \tag{17}$$

Where a is the development coefficient.
The matrix is:

$$B=\begin{bmatrix} -1/2\left(x^{(1)}(1)+x^{(1)}(2)\right) & 1 \\ -1/2\left(x^{(1)}(2)+x^{(1)}(3)\right) & 1 \\ \cdots & \cdots \\ -1/2\left(x^{(1)}(47)+x^{(1)}(48)\right) & 1 \end{bmatrix},\quad Y_N=\begin{bmatrix} x^{(0)}(2) \\ x^{(0)}(3) \\ \cdots \\ x^{(0)}(40) \end{bmatrix} \tag{18}$$

Remember that the parameter is
The following differential equation for the initial conditions:

$$\hat{x}^{(1)}(k+1)=\left(x^{(1)}(1)-\frac{u}{a}\right)e^{-ax}+\frac{u}{a} \tag{19}$$

To reduce it to a predictive model:

$$\hat{x}^{(0)}(k+1)=\hat{x}^{(1)}(k+1)-\hat{x}^{(1)}(k)=e^{-ax}\left(1-e^{a}\right)\left(x^{(0)}(1)-\frac{u}{a}\right) \tag{20}$$

Finally, a posteriori C is used to test the model.

4.4.2 Results of the model

We use MATLAB to solve the model, the results are as follows:

Table 6: The results of the model

year	Precipitation /mm	Change in sea level over year /mm	Drain pipe length /km	Total reservoir capacity / 10,000 cubic meters	Permanent population / 10,000	GDP / 100 million yuan
2023	2040. 2	76	58317	846. 43	5684. 39	7055
2024	1638. 4	48	58411	861. 55	6801. 00	2848
2025	2464. 5	75	58909	876. 83	7806. 54	49305
2026	1719. 5	91	60021	891. 23	8201. 23	1645
2027	1713. 1	64	61139	1035. 70	9510. 91	3255
2028	1713. 1	93	61241	1046. 74	11502. 06	813
2029	1812. 1	153	61365	1054. 74	12950. 10	40772

4.5 Task 4: A report on the triple la Nina Incident

4.5.1 The causes of La Nina

La Niña is associated with cooler water temperatures and stronger trade winds in the equatorial central and eastern Pacific. Therefore, La Nina is actually the product of the interaction of tropical ocean and atmosphere. In the equatorial middle-east Pacific, the atmosphere and the ocean are coupled by the exchange of heat, water vapor and momentum at the interface, and the movement of the ocean surface is mainly controlled by the sea surface wind. Equatorial (easterly) winds from the northern and southern hemispheres blow warm surface water westward, increasing the depth of the 20 ° C isotherm in the western Pacific subsurface, it also provides energy for convection and uplift of the air over the Asian and Indonesian Islands, and the upper air currents return to the eastern Pacific Ocean and sink to form the tropical Wouk circulation.

When the La Niña event occurs, the equatorial trade winds will further strengthen, the cold water upwelling in the coastal ocean of Peru will continuously strengthen, and the tropical zonal circulation will significantly strengthen; when the El Niño event occurs, the equatorial trade winds will weaken, the deep convective zone over Asia and Indonesia moved eastward to form the opposite Walker circulation. In the past 100 years, the LA niña-el Niño cycle has become the strongest natural climate oscillation and the most important precursor signal in seasonal and interannual climate prediction. The cycle of air-sea interaction in the equatorial Middle East Pacific Ocean is generally 2-7 years with an average of 4 years. Further studies show that the East Pacific has a cycle of 3 to 7 years, while the central Pacific has an average cycle of 2 to 3 years. In the 20th century, there were 23 El Niño events and 22 La Niña events. In the 21st century, there have been 7 El Niños and 6 La Niña events, currently experiencing the 7th La Nina event, the 2021 is about to become “Double la Nina Year.”. With the aggravation of global warming, there has been only one strong cold event since 1951, but three Super El Niño events have been recorded.

4.5.2 La Nina triggers regional or global climate anomalies

Why is the persistent anomaly of large-scale sea surface temperatures in the equatorial Middle East Pacific causing a series of extreme weather events on a global scale? The anomalous ocean phenomena trigger the anomalous atmospheric circulation through the tropical air-sea interaction, resulting in the occurrence of anomalous climatic events. Because the warm water continuously heats the atmosphere and forms an updraft, the cold water area forms a vertical downdraft, and the change of the position of the cold and warm sea water area changes the original law of the atmosphere movement, thus causing the climate anomaly, but the mechanism is different in different regions. Although La Niña's impact on global climate anomalies is not as severe as the famous El Niño, its social and economic impact is significant.

The influence of La Nina event on North and other places is mainly transmitted by downstream effect and atmospheric teleconnection. In winter, near the Tropic of Cancer on the northern side of the sinking zone of the equatorial central-eastern Pacific, there is an increase in the activity of Intertropical Convergence Zone convection and an increase in the North Pacific blocking high and good weather system, development of low-value bad weather systems in the Northeast Pacific and west coast of North (good weather systems are controlled by a high-pressure system, with sunny, cloudless, and fine weather; conversely, bad weather systems are controlled by a low-pressure system, with active convective systems, and are prone to weather phenomena such as precipitation) , the southern United States experienced a dry, warm winter; conversely, the El Niño event brought heat and drought to the west coast of North America, and snowstorms to the northeast.

The influence of La Niã ± a event on East Asia is mainly through controlling the location and intensity of the western Pacific Horse latitudes and influencing the East Asian monsoon circulation. Due to the intensification of the tropical Intertropical Convergence Zone convection in the Asian and Indonesian Islands, the northern position and intensity of the western Pacific Horse latitudes are on the strong side, which is conducive to the increase of autumn and winter precipitation in the northern part of our country, forming autumn floods in the north and Hwaseo. At the same time, the East Asian winter monsoon is stronger and the cold air is more active in winter and spring. But El Nino event, makes the southern flood season precipitation on the side. The influence of La Niña event on the tropical areas outside the Pacific Ocean is mainly controlled by the anomaly of the zonal secondary circulation, with frequent torrential rain and flood in northern South and increased flood risk in northern Australia and Southeast Asia. On a global scale, la Nina causes lower temperatures and more precipitation, but it varies from country to country and region to region. When La Niña occurs, there is little precipitation along the coast of South (such as Argentina) , and more rain in Indonesia and eastern Australia; when La Niña lasts for a long time, places such as Central and Southeastern United States Africa are prone to droughts, while north-east Brazil, India and southern Africa are prone to floods

5 Sensitivity Analysis

Since the selected indicators are subjective, we add two new indicators in order to make the model more accurate. And re-solve the model to derive the latest top 20 years compared with the 20 years obtained from the previous solution to obtain the new top 20 years and the years that fell out of the top 20 as:

Table 8 Year of promotion and fall out

Year of promotion	Drop out year
2003	2016
1989	2011
2001	1987
1997	2007
1998	1988

From the table, we can see that the change in ranking is not significant after the addition of new indicators. Therefore, we think that the model based on factor analysis is more stable.

6 Model Evaluation and Further Discussion

6.1 Strengths

(1) In this paper, the selection of indicators in the more comprehensive thinking, and through the analysis of variance and principal component analysis and other ways to select the indicators. Therefore, the model is more reasonable.

(2) The establishment of the model is in accordance with the thinking of solving the problem, we first analyze and find the existing law, then evaluate the existing law, according to the evaluation criteria to build a new model, level gradually easy to understand.

(3) The hypothesis of the model is reasonable, so the model can be built accurately, can better accord with the actual situation, has strong application ability, can be closely linked with the actual situation, combined with the actual situation to solve problems.

(4) For the established judgment tree, we carried on the examination, obtained our judgment tree's correct rate is 90% , the correct rate is higher.

(5) The model has high reliability, strong generalization ability, originality and innovation in solving the problem of basic education status evaluation, and can be applied to real life.

6.2 Weaknesses

(1) The disadvantage of this model is that the method used is relatively simple, and no other method is used to verify the result, if time is enough, we can use fuzzy comprehensive evaluation or principal component comprehensive evaluation to solve the problem.

(2) The data source of this paper is limited, the model accuracy cannot be further evaluated, the model may have some limitations.

6.3 Model improvements

6.3.1 LSTM network optimization based on particle swarm algorithm

The LSTM model needs to set parameters such as time window size and the number of hidden layer units, etc. The different parameters will affect the prediction performance of the training model, so we need to set appropriate model parameters. The selection of hyperparameters for traditional network models often relies on the results of multiple experiments, which can consume a large amount of and computational resources, so we introduce the particle swarm algorithm to analyse the number of hidden layers of the network, and use the time window size and the number of hidden layer units of the neural network in the LSTM model as the optimisationWe use the time window size and the number of hidden layer units in the LSTM model as the optimisation objects, and use variable adaptation weights to improve the global optimisation performance of the particle swarm algorithm.

$$W = W_{\max} - \left(W_{\max} - W_{\min}\right)\left(\frac{n^2}{n_{\max^2}}\right) \tag{21}$$

Since the particle swarm algorithm is characterized by a stochastic optimization process, in order to find the most number of hidden layers faster and more accurately We divide the area density of the particles.

$$\mu_{POS} \geq \frac{\sqrt{\sum\left(d_{ij}-\bar{d}\right)^2}}{n}; i \neq j \tag{22}$$

where d is the Euclidean distance between the two parameters. We then update the adaptation weight information to determine whether the termination condition is reached, and the optimal value of the optimization target is obtained when the termination condition is reached; finally, the training data is trained and the validation data is predicted, and the average absolute percentage error of the prediction result is used as the adaptation value of each particle to derive the corresponding number of hidden layers.

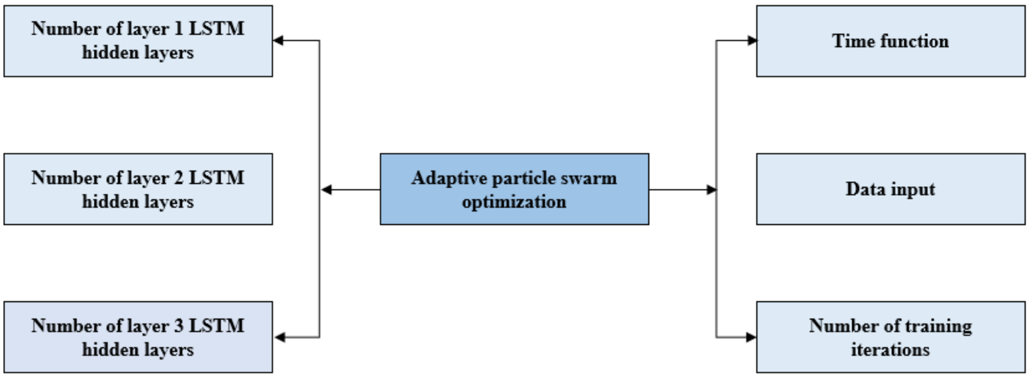

Figure 12: Particle swarm optimization of network structures

7 Conclusion

At present, our country's La Nina/El Niño climate prediction has been among the leading international levels, but the global warming superimposed on the natural climate oscillation of the equatorial middle-east Pacific SST anomaly, extreme weather is widespread, frequent, strong and concurrent, making extreme weather more complex. At present, the BCC-CPSv3 has established a sub-season-season-interannual scale integrated operational climate model forecasting system, which National Climate Center a significant improvement in the performance of climate prediction. The ability of inter-quarterly prediction of El Niño/La Niña events in the Equatorial Middle East Pacific and the east-west SST anomaly structure in the tropical Indian Ocean is also better than that of the United States, the United Kingdom and Japan. A team of Chinese scientists from institutions of Nanjing University of Information Science and Technology and other institutions of higher learning used more than 0.5 percent of their skills to predict an el niño-la niña event 24 months in advance, artificial Intelligence (AI) based on machine deep learning (ml) can be extended to 20 months for predicting the sea surface temperature (SST) of NINO 3.4 area in winter.

References

[1] Yuan Yuan, Shen Lelin, Yan Hongming. Influence of interdecadal La Nina events on winter temperature in Southwest China [J]. Chinese Journal of Geophysics,2022,65(01):169-185.

[2] Notice of the General Office of the Ministry of Agriculture and Rural Affairs on printing and distributing the Plan for Scientific Disaster Resistance and Stable Production and Supply for La Nina This Winter and Next Spring [J]. Bulletin of the Ministry of Agriculture and Rural Affairs, PRC,2021(12):39-42.

[3] Kong Zhaoyang, Zhou Yonghong, Xu Xueqing, An Obviously. Correlation analysis of diurnal length variation, atmospheric angular momentum and ENSO interannual signal and La Nina events from 2020 to 2021 [J]. Advances in Astronomy, 201,39(04):532-543.

[4] Zhang Lijing, Ma Shuang. La Nina stir investment is expected to produce or can be "warm winter" [N]. China securities journal, 2021-11-09 (A05). DOI: 10.28162 / n.c nki. NCZJB. 2021.005407.

[5] Agricultural Products Group, Guangfa Futures Development Research Center. La Nina back Global market or sugar into turmoil [N]. The futures journal, 2021-10-26 (003). The DOI: 10.28619 / n.c. Nki NQHBR. 2021.003433.

[6] Qi Yanwen, Zhao Meilan, Ma Qiang. Analysis on the Failure of climate prediction in Autumn and Winter of Tongliao City in 2020 under La Nina [J]. Weather in Inner Mongolia, 2021 (05) : 23-26.

[7] Wang Xinjian, Liu Yang, Song Lijie. In shandong province, the correlation of climate change and the el nino/la Nina event [J]. Journal of surveying and mapping, Beijing 2021, 35 (6) : 712-716. The DOI: 10.19580 / j.carol carroll nki. 1007-3000.2021.06.002.